Micron 196–197 (2025) 103847

Contents lists available at ScienceDirect

Micron

journal homepage: www.elsevier.com/locate/micron

High-resolution live imaging of tardigrade response to anoxia

Anna-Mari Haapanen-Saaristo [a], Sara Calhim [b], Ilkka Paatero [a,*]

[a] Turku Bioscience Centre, University of Turku and Åbo Akademi University, Turku, Finland
[b] Department of Biological and Environmental Science, University of Jyväskylä, Jyväskylä, Finland

ARTICLE INFO

Keywords:
Fluorescence microscopy
hypoxia
anoxybiosis
tardigrade
intravital imaging

ABSTRACT

Tardigrades are well-known for their ability to tolerate extreme environmental conditions such as heat, drought and lack of oxygen by undergoing cryptobiosis. The molecular responses to stress have been studied in detail, but the physiological and morphogenetic changes during cryptobiosis are less understood. We developed new live high-resolution fluorescence microscopy protocols to visualize the tardigrade response to lack of oxygen – anoxybiosis. High-resolution time-lapse imaging enabled analysis of cellular morphology and tracking of cell movements during anoxybiosis. These analyses revealed considerable changes in morphology, composition and movement of storage cells. Our observations and new imaging protocols can be used to study morphological and cellular response to stress in tardigrades.

1. Introduction

Tardigrades are small aquatic animals, which are known for their ability to withstand extreme conditions (Hashimoto et al., 2016; Møbjerg et al., 2011; Hesgrove and Boothby, 2020). It is notable that these organisms demonstrate remarkable resilience to stress when compared to other animal groups. In contrast to larger organisms, which possess the capacity for extensive migration, small organisms, including tardigrades, are constrained by limited mobility and are therefore compelled to adapt and endure environmental changes (Møbjerg et al., 2011; Nunney, 2016; Momeni et al., 2024).

The ability of tardigrades to survive extreme environmental stressors is based on cryptobiotic states, where metabolic activity is reduced to near-undetectable levels (Guidetti et al., 2011). The phenomenon of cryptobiosis was first documented already in the late 1950s (Keilin, 1959). One of these states is anoxybiosis, induced by a lack of oxygen, which differs from other well-known cryptobiotic forms, such as anhydrobiosis, where survival is facilitated by desiccation. Unlike anhydrobiosis, where tardigrades can remain in a dry, dormant state for years, anoxybiosis is a temporary state of suspended animation that occurs under conditions of severe oxygen deprivation (Hagelbäck and Jönsson, 2023). Once favorable conditions are restored, tardigrades can rapidly recover, resuming normal metabolism and activity (Møbjerg and Neves, 2021).

Investigating anoxybiosis in tardigrades offers unique insights into the cellular and molecular adaptations that allow organisms to endure hypoxic or anoxic conditions. Compared to other cryptobiotic forms, the mechanisms underlying anoxybiosis are less well understood, and while some studies have focused on tardigrades' ability to survive desiccation, far fewer have explored their response to prolonged oxygen deprivation (Hagelbäck and Jönsson, 2023; Møbjerg and Neves, 2021). Responses to anoxic conditions vary among different organisms, including invertebrates such as several species of nematodes (Cox and Gillis, 2020). During oxygen deprivation, some other invertebrates may undergo changes in cellular morphology, including alterations in cellular shape, size, and structure (Miller and Zachary, 2017). These changes are often linked to physiological adaptations, such as reduced metabolic rates and changes in ion transport (Miller and Zachary, 2017; Pedersen et al., 2020; Tattersall et al., 2012). Nevertheless, tardigrades' response to anoxia varies significantly from their other cryptobiotic forms, in which they form a tun (Hesgrove and Boothby, 2020). Tardigrades exhibit a distinctive response to anoxia, a state of oxygen deprivation, which is characterized by a significant increase in body size and the development of elongated limbs. This phenomenon, known as anoxybiosis is a hallmark of tardigrades during periods of anoxia (Hagelbäck and Jönsson, 2023). As the organism undergoes a rapid change in morphology, deviating significantly from the characteristic cryptic state of a tun, it is imperative to elucidate the mechanisms that facilitate cell relocation within the organism's body. The detailed analysis of these mechanisms, however, requires advanced methods such as high-resolution fluorescence microscopy.

High-resolution fluorescence microscopy has become an

* Corresponding author.
E-mail address: ilkka.paatero@utu.fi (I. Paatero).

https://doi.org/10.1016/j.micron.2025.103847
Received 24 January 2025; Received in revised form 7 May 2025; Accepted 7 May 2025
Available online 9 May 2025

indispensable tool in biological research, providing unprecedented insights into cellular structures and physiological processes (Liu et al., 2019; Perry et al., 2015). Unlike conventional light microscopy, high-resolution fluorescence imaging enhances contrast and specificity by utilizing fluorophores that bind to cellular components, enabling precise tracking of structural and biochemical dynamics (Czerneková et al., 2018a; Harry et al., 2024; Heikes and Goldstein, 2018). In tardigrade studies, these imaging techniques would allow for detailed visualization of morphological adaptations, intracellular organization, and metabolic changes under different environmental stressors.

Fluorescence microscopy has already been instrumental in investigating cryptobiosis-related mechanisms in tardigrades. Previous studies have employed fluorescence imaging to examine the distribution and function of stress-related proteins, such as intrinsically disordered proteins (IDPs) involved in desiccation tolerance (Boothby et al., 2017). Additionally, genetically encoded fluorescent markers have been successfully expressed in transgenic tardigrades, expanding the possibilities for in vivo tracking of molecular responses (Tanaka et al., 2023a). Live fluorescence imaging has also enabled researchers to monitor intracellular changes during anhydrobiosis and tun formation, revealing the reorganization of storage cells and metabolic shifts during stress adaptation (Bartels et al., 2024; Beis and Stainier, 2006). These results imply that high-resolution fluorescence live microscopy can be utilized for analysis of mechanisms and dynamics of tardigrade anoxybiosis.

Understanding mechanisms and dynamics of stress responses could illuminate broader ecological implications, particularly as climate change continues to alter habitats, potentially exposing tardigrades to unprecedented combinations of environmental challenges. The elucidation of stress responses of tardigrades has been also proposed to provide novel views of developing medical treatments and therapies (Hesgrove and Boothby, 2020; Giovannini et al., 2022; Wilsterman et al., 2021). In this study, our aim was to develop and use high-resolution fluorescence microscopy methodology for a detailed analysis of the tardigrade's transition into anoxybiosis.

2. Results

2.1. Protocol for live imaging of tardigrade anoxybiosis

Anoxybiosis is species specific adaptation mechanism and there are tardigrade species that tolerate anoxia poorly (Hagelbäck and Jönsson, 2023; Nelson, 2002). The range of toleration can vary from hours to

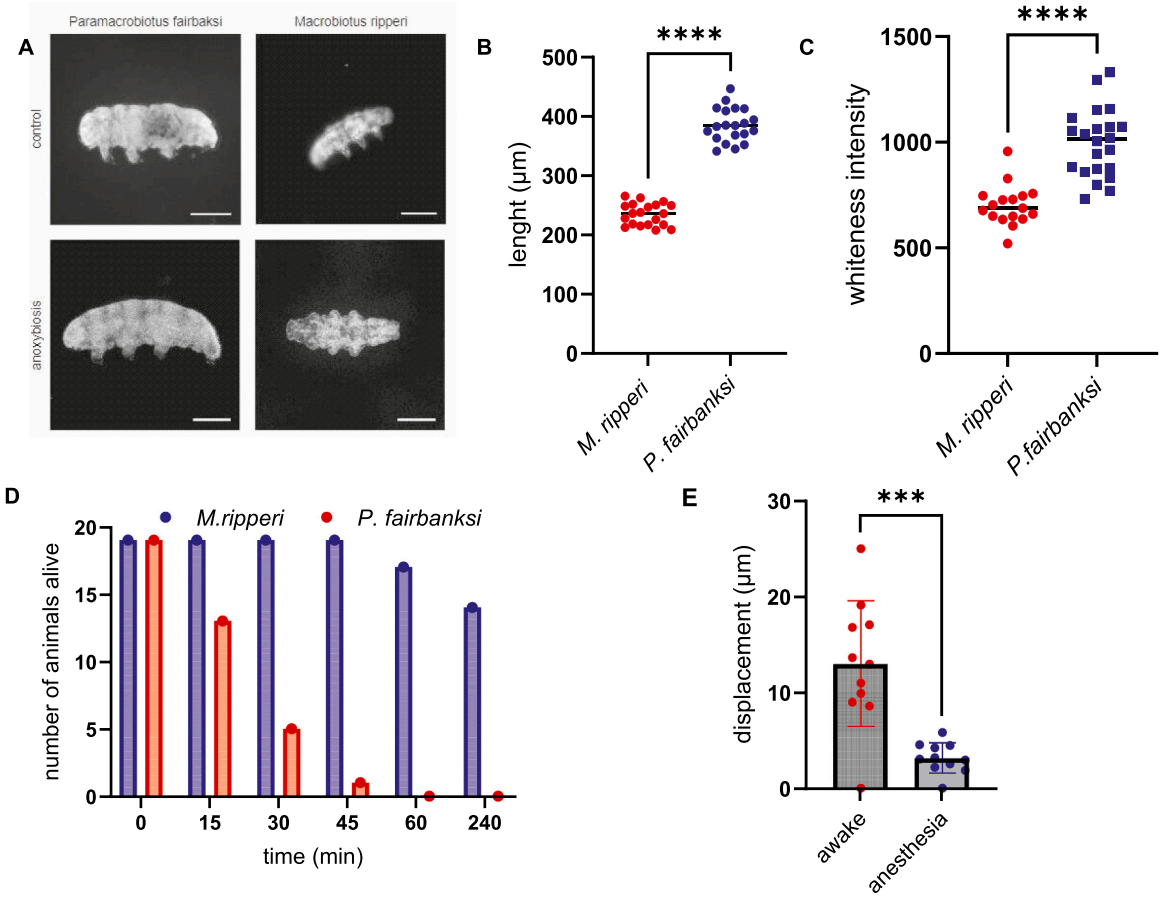

Fig. 1. Finding suitable conditions for imaging studies of anoxia response in tardigrades. **(A)** Reflected light stereomicroscopy images of tardigrades. Anoxybiosis affected the size of tardigrade. Scale bar 100 µm. **(B)** Measurement of length of tardigrades. The two species (*M.ripperi and P.fairbanksi*) were of different length (n_ripperi = 20, n_fairbanksi=20, Mann-Whitney $P < 0.0001$). **(C)** Measurement of volume indicated significant size difference in the animals, *P. fairbanksi* being noticeable bigger (n_ripperi = 16, n_fairbanksi=13, Mann-Whitney $P < 0.0001$) **(D)** Analysis of survival under anoxia. The same groups of tardigrades were observed during 4-hour anoxia exposure and number of living tradigrades was counted in 0, 15, 30, 45, 60 and 240 min time points. *M. ripperi* showed better survival rates compared to *P. fairbanksi*. *P.fairbanksi* did not correspond to chemical hypoxia well, leading to 100 % dead rate after 4-hour exposure (n_ripperi = 19, n_fairbanksi = 19. Log-rank (Mantel-Cox) test $P < 0.001$). **(E)** Analysis of transparency. The increased reflected light intensity of tardigrades imaged against black background under reflected light illumination indicates reduced transparency. A notable disparity in the intensity indicates that *M. ripperi* exhibits greater transparency compared to *P. fairbanksi* (n_(ripperi) = 17, n_(fairbanksi) = 21, Mann-Whitney $P < 0.0001$). **(F)** Analysis of tardigrade movement during live imaging. Short bright-field time-lapse movies or awake and anaesthetized tardigrades were obtained with a stereomicroscope. There was significant decrease in motility when using Tricaine (MS222) as anesthetic. Mann-Whitney unpaired *t*-test $P < 0.0004$, n_ripperi = 5, n_fairbanksi = 5, with 11 measurement points each.

several days (Nelson, 2002). To find a suitable model for anoxybiosis studies we tested two eutardigrade species *Macrobiotus ripperi* (Stec et al., 2021) and *Paramacrobiotus fairbanksi* (Kayastha et al., 2023) (Fig. 1A). *P. fairbanksi* is a larger species and *M. ripperi* is smaller (Fig. 1B-C). *M. ripperi* was able to withstand anoxia better than *P. fairbanksi* (Fig. 1D). In addition to its better tolerance of low oxygen levels, *M. ripperi* was more transparent (Fig. 1E) which was beneficial for the imaging experiments. Some tardigrade species have significant cuticular autofluorescence, which can interfere with fluorescence imaging of internal structures (Bartels et al., 2024). *P. fairbanksi* had stronger autofluorescence than *M. ripperi* in cuticular structures and was opaquer, which was observed as whiter shade (Figs. 1A, 1E). These observations were consistent with earlier findings in *Paramacrobiotus sp* (Suma et al., 2020). Based on the observations of higher transparency, reduced autofluorescence and higher tolerance to anoxia, we decided to continue the studies with *M. ripperi*.

To enable live imaging studies, we needed to develop methods for immobilization of live tardigrades. Embedding of samples into low-melting point agarose is widely used to immobilize small organisms for imaging (Kleinhans and Lecaudey, 2019; Burnett et al., 2017). When we embedded *M. ripperi* in agarose, we observed that agarose alone could not restrain movement of *M. ripperi* sufficiently. Therefore, we tested MS-222 used in zebrafish embryo anesthesia (Leyden et al., 2022) and levamisole, which is used in immobilization of *C. elegans* for live imaging (Qian et al., 2008). Levamisole proved lethal to *M. ripperi*, but MS-222 was well tolerated and significantly reduced the movement of *M. ripperi* (Fig. 1F, supplemental movies S1 and S2). The MS-222 anesthesia together with mounting in low-melting point agarose provided sufficient control for high-resolution imaging experiments.

2.2. Fluorescence staining of live tardigrades

In order to analyze the morphological changes of tardigrades during anoxybiosis, we aimed to identify suitable fluorescent labels. Although the use of genetically encoded fluorescent reporters has been recently demonstrated in some other tardigrade species (Tanaka et al., 2023b), we explored organic vital fluorescent dyes due to easier implementation and flexibility in experimentation. Two dyes previously employed for vital staining of other organisms, acridine orange and Nile red, were observed to label discrete structures in *M. ripperi* (Fig. 2A) with sufficient intensity. The intensity was significantly increased upon long incubations (Fig. 2B), most likely due to slow absorption of dye through chitin-rich outer cuticle of tardigrades. Acridine orange (AO) stains nucleic acids and Nile red (NR) stains lipids (Greenspan et al., 1985; Iessi et al., 2017).

2.3. Tardigrades exhibit rapid changes within the body upon anoxia

The morphology of tardigrades is altered in anoxybiosis (Nelson, 2002). To analyze temporal changes in response to low oxygen levels, we chemically depleted oxygen from the culture medium and imaged *M. ripperi* during transition in anoxybiosis (Fig. 3A). The body length was increased during anoxia and visible increase was observed already in the early stages of anoxic exposure. The fastest rate of body length change was after 25 minutes (Fig. 3B). The volumetric measurements indicated that the alteration was not merely an increase in length, but rather a generalized expansion of the body (Fig. 3C).

2.4. High-resolution live imaging of tardigrades

Next, we carried-out high-resolution experiments using spinning disk fluorescence microscopy, which provides good resolution with sufficient volumetric imaging performance and imaging speed (Wilson, 2010). The imaging with spinning disk confocal in high-resolution resulted in subcellular level resolution within living tardigrades (Fig. 4). For example, storage cells were clearly visible and characterized by strong

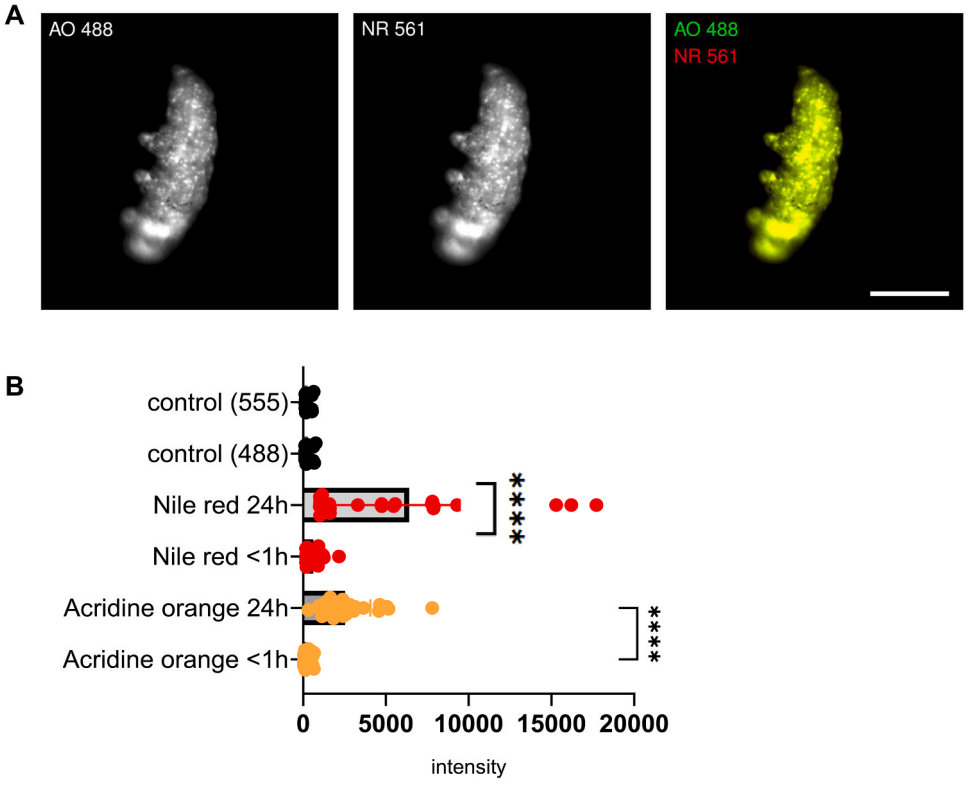

Fig. 2. Vital fluorescent labeling of *M. ripperi*. **(A)** Fluorescent microscopy images of *M. ripperi* stained with acridine orange (AO) and Nile Red (NR) imaged with AxioZoom stereomicroscope. Scale bar 100 μm. **(B)** Quantification of fluorescence intensity. Background is reduced from actual fluorescent measurements (control). Number of tested animals: n(control) = 38, n(NR24h) = 25, n(NR1h) = 27, n(AO24h) = 23, n(AO1h) = 33. Unpaired *t*-test, AO $P < 0.0001$ and NR $P < 0.0001$.

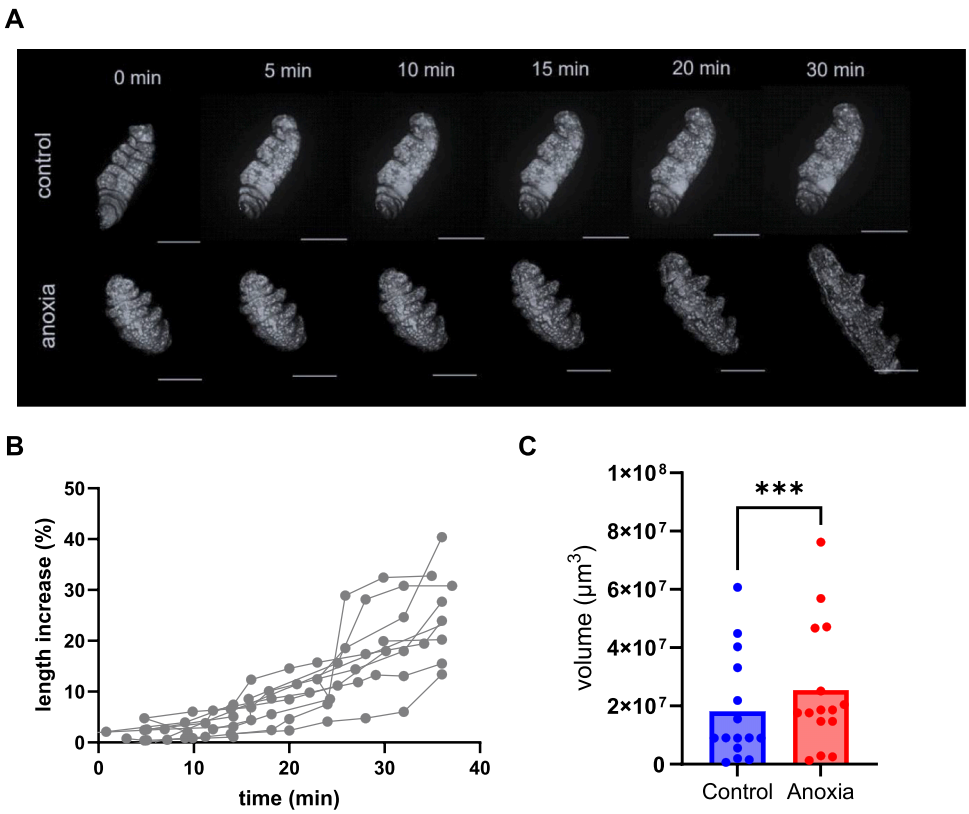

Fig. 3. During anoxybiosis the body volume of tardigrade increases. **(A)** Time-lapse imaging and maximum Z-projection visualized the difference between tardigrade in normal oxygen levels and when exposed to anoxia. Scale bar 50 µm. Spinning disk confocal imaging. **(B)** Measurement of body length during anoxybiosis. The length of tardigrade was normalized to its size at the beginning of each movie. n = 8. Used light sheet (FLSM) and spinning disk confocal data. **(C)** Volume measurements of 3D imaged tardigrades. Paired *t*-test, p = <0.0001, n = 15. FLSM and spinning disk confocal data.

NR signal. Storage cells are a specialized cell type of tardigrades, carrying rich lipid energy reserves (Czerneková et al., 2018b), which is consistent with observed strong NR signals. Sufficient resolution was required for down-stream image analysis and especially for segmentation and tracking.

2.5. Anoxia increases the movement of storage cells

Some studies have showed the importance of storage cells in recovery from environmental stress (Czerneková et al., 2018a; Reuner et al., 2010). We hypothesized that storage cells could have an active role during anoxybiosis. To quantitatively analyze cellular movements of storage cells during transition into anoxybiosis, we utilized spinning disk confocal fluorescence time-lapse 3D imaging of tardigrades. From the 3D time-lapse imaging data, we segmented storage cells (stained lipids with Nile Red) and carried out tracking analysis to measure diverse parameters of cellular dynamics of the expanding body of tardigrade (Fig. 5A, supplemental Figure S1). The total number of tracks observed was significantly lower in animals belonging to the control group. This could have resulted from decrease in overall cellular movement in response to oxygen deprivation, segmentation quality or one factor is projected data in order to run the heavy pipelines in Fiji software. Besides the amount of tracks we observed that the duration of the tracks was lower in anoxia groups (Fig. 5B). We hypothesized that the passive swelling of the animal would result in increased total distance travelled, increased straight line speed, increased displacement, increased confinement ratio and reduced mean directional change. The total distance travelled (Fig. 5C), mean speed of cells (Fig. 5D) and straight-line speed (Fig. 5E) were increased in anoxia, as expected. However, the measurements of confinement ratio (Supplemental figure S2A) or displacement (Supplemental figure S2B) did not exhibit statistically significant differences between the anoxia-exposed group and the control group. This suggests that the spatial confinement of cellular movement remained relatively consistent under both conditions. Mean directional change indicates a greater degree of directional changes in cell movement over time reflecting increased cellular exploration or response to environmental cues. Taken together, this data implies that morphological changes in anoxybiosis are not just caused by passive swelling, but may involve active movement of storage cells.

2.6. Anoxia alters storage cells

To address the hypothesis that storage cells may have active role in anoxybiosis, we analyzed morphology of these cells in detail using high-resolution imaging (Fig. 6A). The analysis of storage cell morphology over time indicated that during anoxia the cell size increased, (Fig. 6B), but their rounded cellular shape did not significantly change (Fig. 6C).

Serendipitously, we also observed that the NR intensity increased during anoxybiosis (Fig. 6D). NR has interesting solvatochromic properties and it generates stronger red fluorescence when bound to polar rather than non-polar organic solvents (Greenspan et al., 1985). This implied that storage cells underwent metabolic changes during anoxybiosis and their lipid metabolism and constitution was altered. Lipids are typically stored as triacylglycerols (TAG) and metabolized into non-esterified free fatty acids (NEFA) for utilization in beta-oxidation metabolic cycle (Hauton et al., 2001). This process not only generates energy but also transforms lipids from non-polar form into more polar structures (Suma et al., 2020; Wilson, 2010), consistent with increase of NR fluorescence during anoxybiosis. Taken together, our findings illustrated changes of storage cell movement, morphology and composition during anoxybiosis, indicating active role of storage cells during anoxybiosis.

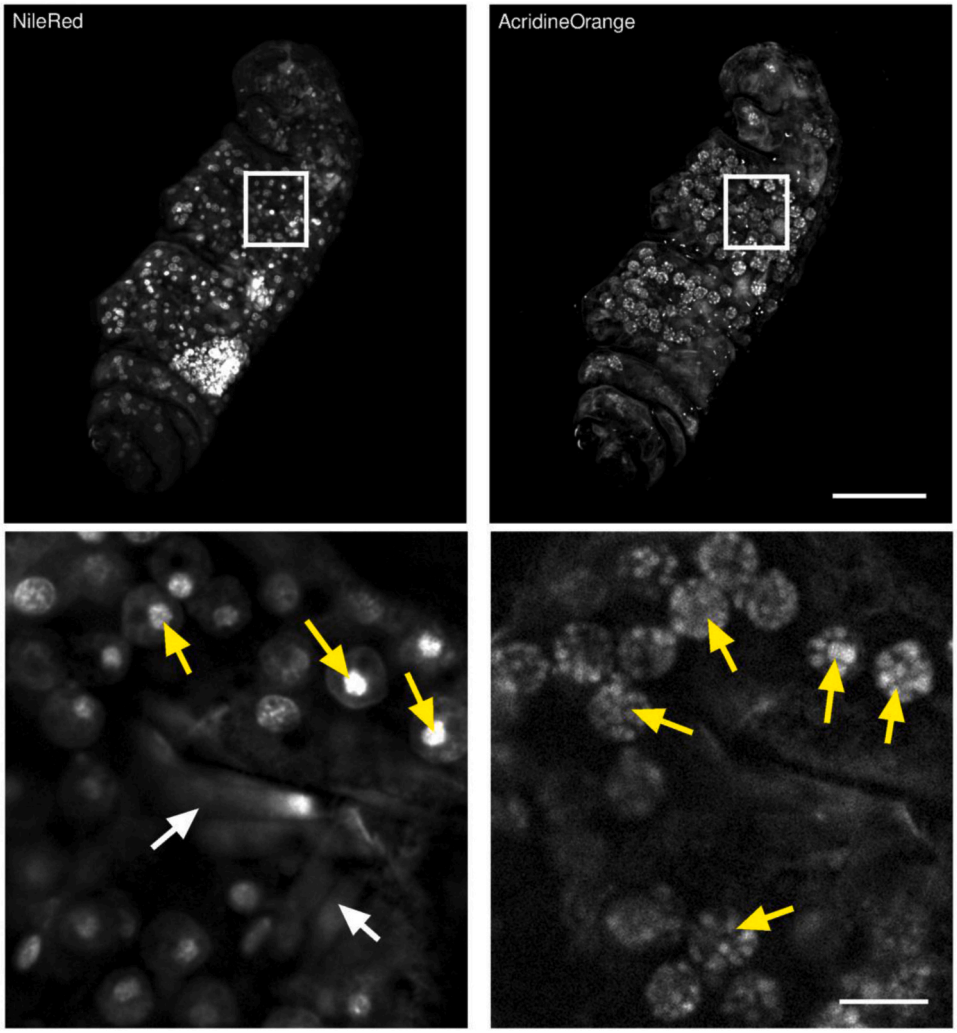

Fig. 4. Higher-resolution spinning disk confocal imaging of tardigrades. Spinning disk confocal provided high resolution fluorescence imaging and enabled investigations of change in internal structures of the animal. Yellow arrows annotate storage cells, and White arrows annotate the muscular structures. Scale bar 50 μm / 10 μm.

3. Discussion

In this study, we investigated the morphological changes of tardigrades during anoxybiosis by developing live fluorescence imaging protocols and using high-resolution and intravital imaging technologies.

First, we observed that two tardigrade species *P. fairbanksi* and *M. ripperi* had different sensitivity to anoxia. This aligns with previous findings that tardigrade species exhibit distinct survival capacities under oxygen deprivation (Nelson, 2002; Keilin, 1959). For example, the *Richtersius* cf. *coronifer* and *Hypsibius exemplaris* responded to hypoxia differently: both species exhibited irregular body movements at similar oxygen levels, but larger fraction of *R.* cf. *coronifer* regained regular movements after 10 hours of recovery from hypoxia (Hagelbäck and Jönsson, 2023). The oxygen depletion by using sodium metabisulphite has potential to affect oxidation-reduction potential (ORP) of the solution. In our hand, the ORP was reduced but stayed clearly on the oxidative level (+159 mV) even after oxygen depletion. The ORP level was not significantly different from naturally occurring variation (Barczok et al., 2023; Stefánsson et al., 2005), and therefore unlikely to cause significant effects on the tardigrades in these experiments. In the nature, the oxygen depletion may occur through reductive biological and chemical processes, which is consistent with reduced ORP in our experimental setting. The dissection of the relative importance of oxygen and ORP on anoxybiosis would be an interesting area for future studies.

The utilization of high-resolution imaging has afforded us an unprecedented level of detail in observing the structural alterations in tardigrades undergoing anoxybiosis. These techniques have demonstrated the preservation of cellular integrity and the morphological adaptations that can explain tolerance for anoxic conditions. The observed changes in cuticle structure (expansion, swelling), the reorganization of cells (storage cell movement), and the alterations of metabolism within storage cells (lipids) may be linked to survival mechanisms. Studies that have investigated cryptobiosis in general have pointed out storage cells and their function related to stress tolerance (Keilin, 1959; Halberg et al., 2012). The storage cells are considered to function as the energy storages of tardigrades (Czerneková et al., 2018b; Reuner et al., 2010; Quiroga-Artigas and Moriel-Carretero, 2023), but these cells may have also other roles such as in vitellogenesis (Hyra et al., 2016). In anhydrobiosis, there is increased expression of genes belonging to the SAHS (secretory abundant heat-soluble) family in storage cells hinting at their potential involvement in desiccation tolerance (Tanaka et al., 2023b). Our experiments implied changes in tardigrade metabolism in anoxybiosis, indicated by intensity changes of NR dye. Advanced imaging modalities such as mass spectrometry imaging or CARS (Coherent Anti-Stokes Raman Scattering) microscopy could later provide deeper information of metabolic responses of tardigrades to anoxic conditions. The importance of further investigation of tardigrade metabolism has

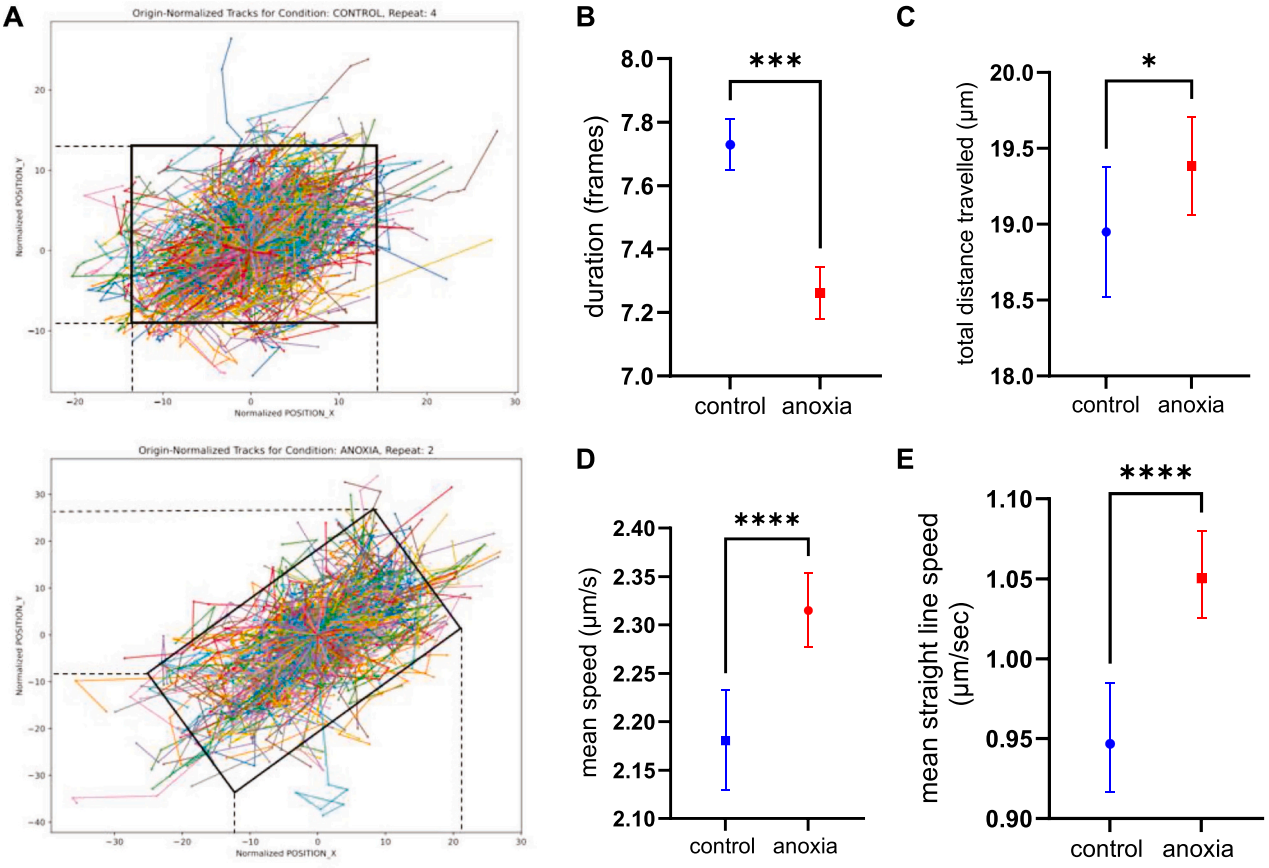

Fig. 5. Tracking measurements. All together 5 anoxia and 5 control animals which were exposed to anoxia for 40 minutes, imaged by spinning disk confocal with 4-minute intervals. Tracking was performed with ImageJ for image set that were converted maximum intensity projections to reduce computational burden of the tracking pipeline. Total number of tracks in control group was 1963 and in anoxia the number of tracks was 3657. Data was pooled to reduce the error caused by individuality. **(A)** Visualization of track movement both in control and experimental animal. For the analysis CellTracksColab was used. **(B)** Analysis of duration of tracks. Duration of tracks showed within the anoxia group the tracks lasted shorter period. Mann-Whitney $p = 0.0007$. **(C)** Analysis of total distance traveled. Longer paths of the cells in anoxia group were observed. Mann-Whitney $p = 0.0231$ **(D)** Analysis of mean speed. Mean speed (µm/s) was clearly higher in anoxia tracks which was expected. Mann-Whitney $p = <0.0001$. **(E)** Analysis of mean straight line speed. Mean straight line speed was higher in anoxia Mann-Whitney $p = <0.0001$.

been emphasized (Hagelbäck and Jönsson, 2023) as it still has many open questions.

We developed protocols for live imaging of tardigrades using fluorescent dyes and high-resolution imaging. On the other hand, recent work has described protocol to make fluorescent transgenic tardigrade models (Tanaka et al., 2023b), which can facilitate future studies of molecular functions and interactions during cryptobiotic processes. During the preparation of this article also the use of some other fluorescent dyes in imaging of tardigrades was reported in Ref (Harry et al., 2024). In addition, fluorescence shadow imaging can be utilized to image external morphology of tardigrades (Flinn et al., 2024). These methods are complimentary to each other, and together expand the experimental toolbox available to study tardigrade biology (Coste et al., 2020; Beis and Stainier, 2006). By correlating detailed structural observations with dynamic physiological processes, we can begin to construct a comprehensive picture of how tardigrades manage to halt metabolic processes and protect cellular components during anoxia, only to resume normal physiological functions upon reoxygenation.

Intravital imaging complemented high-resolution static imaging by providing a dynamic view of the tardigrade's response to anoxia. Techniques such as live-cell fluorescence microscopy have enabled the real-time tracking of physiological processes, including the redistribution of intracellular components (Pittet and Weissleder, 2011). Moreover, intravital imaging allowed for the study of tardigrade behavior and physiology in a more natural context, facilitating future studies on how environmental factors influence the onset and termination of anoxybiosis. The insights gained from our study extend beyond the biology of tardigrades, offering valuable lessons for the broader field of extremophile research. Elucidation of survival mechanisms in inhospitable conditions is relevant not only for evolutionary biology and ecology but also has potential applications in biotechnology and medicine (Greenspan et al., 1985). It has been proposed that the understanding mechanisms of stress tolerance could lead to innovative strategies for preserving cells and tissues in medical settings or developing life-support systems (Kasianchuk et al., 2023).

In conclusion, the utilization of high-resolution and intravital imaging in the investigation of tardigrade anoxybiosis facilitated the acquisition of novel insights that may elucidate the underlying mechanisms of extreme survival strategies. Our findings also support further study of the components that take part when tardigrades are exposed to different oxygen levels. Because anoxybiosis differs from cryptobiotic forms that rely on tun formation, we consider the deeper understanding of what happens with storage cells during and after anoxybiosis vital. As these imaging technologies are harnessed and further developed, it enables uncovering new biological wonders and deepening our understanding of the resilience of life in the face of adverse conditions.

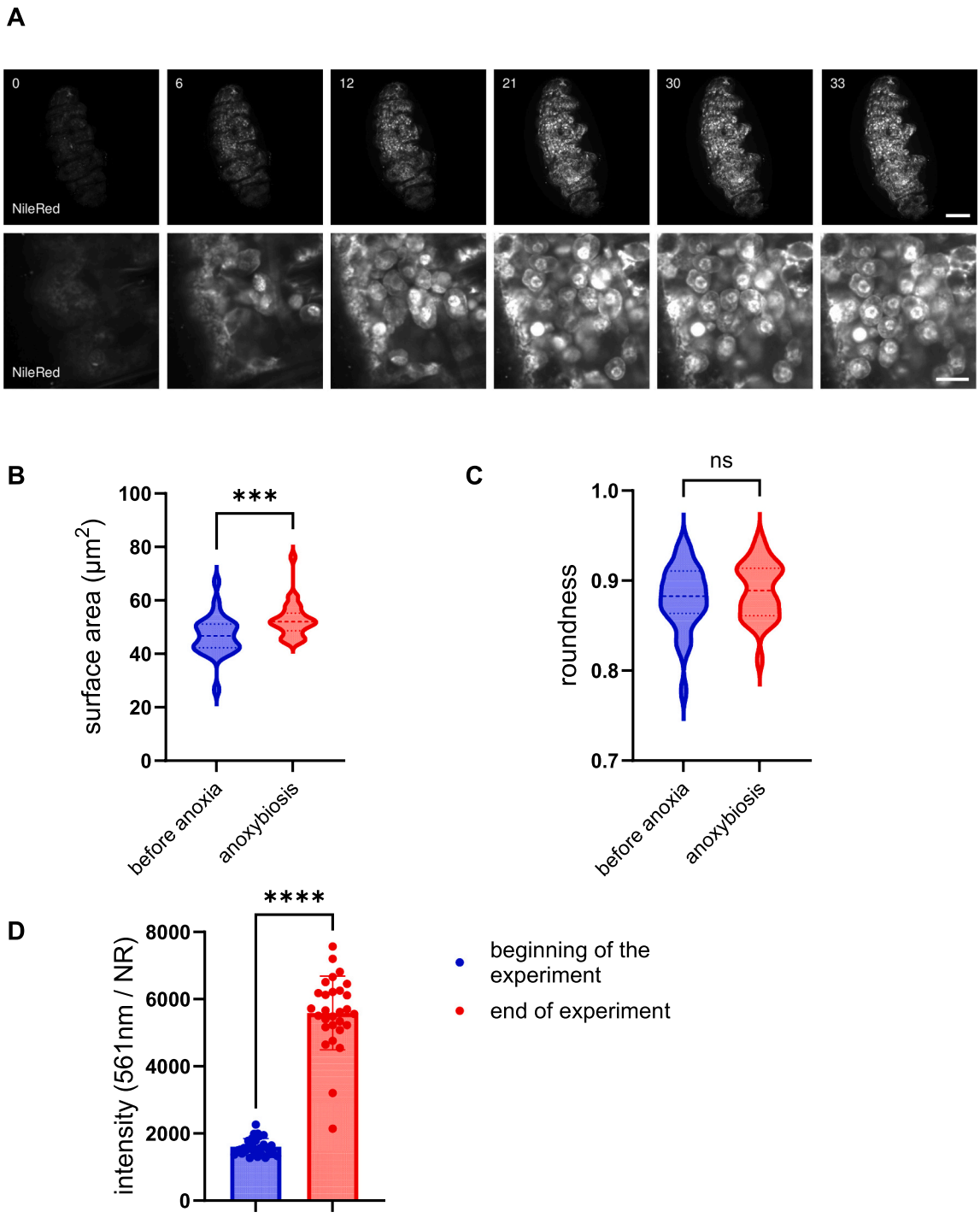

Fig. 6.. Investigation of storage cells. **(A)** *M. ripperi* stained with Nile Red and Acridine orange imaged with time-lapse high-resolution spinning disk confocal imaging. Whole-animal in upper row and close-up presented in lower row. Scalebar 50 µm in upper row. and 10 µm in lower row. Time in minutes. Five animals were imaged. **(B)** Quantitation of the surface area of storage cells. We measured manually the surface area of the cells, used plane in z-stack which provide the largest cell diameter to be measured, in timepoint zero and in full anoxybiosis. Mann-Whitney test, P = 0.0006. n = 25 (per time point). **(C)** Quantitation of the shape of storage cells. We measured the outline of the cells in timepoint zero and in full anoxybiosis. Roundness was used as quantitative measure for shape. Mann-Whitney, P = 0.45 n = 25 (per time point) **(D)** Measurement of NR fluorescence intensity. Intensity of NR was measured from individual storage cells using excitation at 561 nm. Mann-Whitney, P = 0.0001. n = 139 (before anoxia), n = 140 (anoxybiosis).

4. Materials and methods

4.1. Tardigrade culture

Macrobiotus ripperi collected from moss in Jyväskylä, Finland in 2014. Animals were cultured in high wall plastic petridish (⌀50 mm, height 20.3 mm) (Sterilin™ Petri Dishes, Thermo Scientific). The dish was scratched with sandpaper for the animals to be able to walk on the surface. Spring water (Kotimaista lähdevesi, Multiala spring, Finland) was used as medium, and animals were fed with RG Complete (Planktovie SAS, Marseille, France) and young *Panagrellus pycnus* nematodes (laboratory cultured, batch gained from University of Jyväskylä).

Incubator was set on 18°C. No light-dark cycle was applied. Animals were imaged weekly with Zeiss Stemi 350 stereomicroscope (Carl Zeiss AG, Oberkochen, Germany) to monitor culture quality, feeding and cleaning.

4.2. Testing the anesthetic

Testing the anesthetics was performed by applying the anesthetic on agarose mounted tardigrades. The effect was observed and imaged by Zeiss AxioZoom stereomicroscope. All together 25 *M. ripperi* and 23 *P. fairbanksi* were used at timepoints: 15 minutes, 30 minutes, 1 hour and 4 hours. Concentrations of anesthetic solutions of Levamisole was 0.5 mg/ml and MS-222 was 2 mg/ml. The animals were considered dead if there were no signs of recovery (motility and normal morphology) after 24 hours after removal of anesthetic.

4.3. Tardigrade staining, anesthesia and anoxia solution

The animals were stained 24 hours in a total volume of 2 ml of staining solution. The dyes were prepared by diluting 1 mg/ml stock solution acridine orange (ThermoFischer Scientific, Germany) in spring water and 10 mg/ml stock solution NileRed (Sigma Aldrich, Germany) in DMSO. Resulting concentrations varying from 5 μM to 10 μM. Prior to imaging, the animals were rinsed in order to eliminate any residual dye. Acridine orange was employed for comprehensive labelling of the nuclei. Additionally, the dye imparts a yellowish hue to the entire animal, which facilitates detection, particularly in light sheet imaging. Nile Red was used to stain lipids in storage cells. The dyes exhibit slight spectral overlap, yet this did not necessitate any adjustments in our studies due to their structural specificity.

The animals were mounted in low-melting-point agarose (Sigma Aldrich, Germany) and positioned on either a silicon sample holder for light sheet imaging or a glass bottom dish with inverted microscopes, such as a spinning disk confocal. The animals were anaesthetized with 2 g/l tricaine (MS222, Sigma Aldrich, Germany). This was selected over levamisole due to the higher survival rate. Once the mounting process was complete, the animals were ready for imaging. Following imaging, the animals were transferred to fresh spring water to recover.

For chemical anoxia, sodium metabisulfite (JT Baker, ThermoScientific, Germany) was used. The concentration of sodium metabisulfite in the anoxia solution was 1 mg/ml. Oxygen levels of the solution were tested with JBL ProAquatest O2 (JBL GmbH & Co. KG, Neuhofen, Germany), and was at/below detection limit (<0.2 mg/ml) of the test. Sodium metabisulfite decreases the pH which corrected to match the spring water (pH 6.5) with 1 M NaOH. Anoxia solution was pipetted on the agarose in large excess. The potentiometric oxidation-reduction potential (ORP) measurements were performed using a Lawson Labs EMF 16-channel multi-voltmeter (Malvern, PA, USA). A platinum (Pt) electrode, and Metrohm single junction Ag/AgCl/3 M KCl (6.0733.100, Switzerland) were used as the indicator and reference electrode, respectively. The ORP difference between pure spring water and anoxic water was moderate, approximately 205 mV (pure water 364 mV and sodium metabisulfite dissolved in water: 159 mV). Both conditions had positive ORP indicating oxidizing conditions. As control, we also measured the intensity of Nile red during imaging in normoxic and anoxic spring water in vitro placed in agarose in the absence of tardigrades. The Nile red intensity was reduced by –1 + /-4 % in normoxic and increased by 12 + /-9 % in anoxic spring water during imaging. This indicated that the change in ORP had minimal effect for live imaging experiments.

Control groups were handled the very same protocol except the chemically applied anoxia exposure.

4.4. Light-sheet imaging

Light sheet fluorescent microscope (M2 Aurora Airy beam, M Squared Life, Glasgow, UK) was used in intravital imaging of tardigrade anoxybiosis. Tardigrade was mounted on a single drop (~10 μl) of 1.2 %-1.5 % agarose on a silicon sample holder and set in the imaging chamber filled with anoxia solution (J.T.Baker, FisherScientific, Germany). MS222 was used to anesthetize the animal before anoxic treatment to make sure the position is beneficial for the imaging.

Excitation and detection objectives (Special Optics) provided magnification and numerical aperture value based on imaging media. The media was water / agarose. The refractive Index (RI) of water was 1.33, reaching magnification up to 16x with NA0.4 and resolution up to 2.35 pixels / μm, optical resolution of 0.6–0.7 μm, with up to 870 μm x 870 μm full field-of-view. In some cases, we used smaller field-of-view for optimal data collection. In time lapse imaging, a full 3D-stack was collected with 4-minute intervals for 40 minutes.

4.5. Spinning disk imaging

Spinning disk (multi-point) confocal microscope (3i Marianas CSU-W1 spinning disk, Denver, Colorado, US) was used to gain high resolution images of tardigrades. Sample preparation included agarose mounting on a glass bottom dish, anesthesia and anoxia treatment with experimental animals. Imaging settings were straight forward; excitation lasers 488 nm and 561 nm, fixed filters and camera Hamamatsu sCMOS Orca Flash4.0 2048 × 2048 pixels, 6.5 × 6.5 μm and 40x NA1.1 Zeiss LD C-Apochromat WI objective with working distance of 620 μm. Optical resolution with 561 nm laser reaches up to 0.225 μm. With 40x objective our FOV is 325 μm x 325 μm so one animal fit in, camera resolution up to 6.3 pixels/μm. Time lapse imaging was set to 4-minute intervals for 40 minutes.

4.6. Stereomicroscope imaging assays

Motility studies carried out with Zeiss AxioZoom.V16 stereomicroscope with 1 × 0.125 objective (Carl Zeiss AG, Oberkochen, Germany). Short bright field videos were captured with Zeiss movie maker and tardigrades manually tracked using Manual Tracking (Fiji /ImageJ, Wayne Rasband and contributors, NIH, USA) in the presence and absence of anesthetic. Initial testing of fluorescent dyes was done with Zeiss AxioZoom using filters Alexa 488 - filter set 38 HE and Alexa 568 - filter set 45.

4.7. Cell tracking

For cell tracking of spinning disk data, we used Fiji Trackmate (Ershov et al., 2022). With larger data sets (i.e., light sheet) we used Zeiss Arivis Vision 4D 3.5 (Zeiss Group, Oberkochen, Germany) for particle detection and tracking. CellTrackColab (Gómez-de-Mariscal et al., 2024) was used for deeper analysis of the Trackmate defined tracks of confocal spinning disk images sets.

In Fiji Trackmate, we used LoG detection for 2 × 2 binned image sets. Estimated object diameter was set 10 μm and threshold 30; these values were used for every image sets. For tracking Simple LAP tracker, max distance was set to 30 μm, same as gap closing. Max frame gap was set to 2, however the 2-spot tracks were filtered out in later analysis steps.

In Arivis we used analysis panel to create pipeline for tracking cells and particles. Common workflow included setting up the detection for desired channels (lipids for Nile red and overall tracking with AO). Additional parameters included background correction, morphology filter and shape detection. To improve segmentation, we also applied either intensity-based watershed or machine learning based segmentation.

4.8. Volume measurements

3D renderings for volume measurements were done using Imaris

(Bitplane, South Windsor, CT, USA). These are estimations extrapolated from composite images. After image file format conversion, the Surface module was used and threshold was set manually. 3D renderings were carried out with Zeiss Arivis as well. For volume approximations a tardigrade's body is roughly an ellipsoid, so the volume can be estimated from 2D data using: $V \approx (4/3)\pi \times (L/2) \times (W/2)^2$, in which L is length of the animal and W is width of the animal.

Statistical analyses

The statistical analyses were conducted using GraphPad Prism (version 10.1.2 for Windows, GraphPad Software, Boston, Massachusetts, USA; www.graphpad.com). Non-parametric Mann-Whitney analyses and t-tests were conducted for non-normal and normally distributed data, respectively. The survival data were analyzed using the Mantel-Cox log-rank test. The CellTrack Colab data were analyzed on the server and randomizations were based on the experimental nature of the data. The image files were packed in max projection format for lighter processing. The settings were consistent across all data sets, ensuring that any errors were adjusted correctly for the entire data set.

Funding

University of Turku (I.P.), BusinessFinland (1718/31/2021), Finnish Foundation for Cardiovascular Research (230066).

CRediT authorship contribution statement

Haapanen-Saaristo Anna-Mari: Writing – review & editing, Writing – original draft, Visualization, Validation, Methodology, Investigation, Formal analysis, Conceptualization. **Paatero Ilkka:** Writing – review & editing, Writing – original draft, Supervision, Resources, Project administration, Methodology, Funding acquisition, Formal analysis, Conceptualization. **Calhim Sara:** Writing – review & editing, Supervision, Resources, Funding acquisition, Conceptualization.

Declaration of Competing Interest

The authors declare the following financial interests/personal relationships which may be considered as potential competing interests: Ilkka Paatero reports financial support was provided by Business Finland. Ilkka Paatero reports financial support was provided by Finnish Foundation for Cardiovascular Research. University of Turku has registered trademark 3DFLUOHISTO®, and I.P. is involved in the commercialization of 3DFLUOHISTO-technology. Other authors declare that they have no conflict of interest. If there are other authors, they declare that they have no known competing financial interests or personal relationships that could have appeared to influence the work reported in this paper.

Acknowledgements

We would like to express our gratitude to Cell Imaging Core and Zebrafish Core of Turku Bioscience Centre, supported by Biocenter Finland, for their invaluable support, infrastructure and resources.

Competing interests

University of Turku has registered trademark 3DFLUOHISTO®, and I.P. is involved in the commercialization of 3DFLUOHISTO-technology. Other authors declare that they have no conflict of interest.

Appendix A. Supporting information

Supplementary data associated with this article can be found in the online version at doi:10.1016/j.micron.2025.103847.

Data Availability

Data will be made available on request.

References

Barczok, M., Smith, C., Di Domenico, N., Kinsman-Costello, L., Herndon, E., 2023. Variability in soil redox response to seasonal flooding in a vernal pond. Front Environ. Sci. 11, 1114814. https://doi.org/10.3389/fenvs.2023.1114814.

Bartels, P.J., Coffey, D.C., Pineau, M., Kaczmarek, Ł., Nelson, D.R., 2024. An exploration of autofluorescence in tardigrades (phylum Tardigrada). Zool. J. Linn. Soc. 200 (1), 200–217. https://doi.org/10.1093/zoolinnean/zlad045.

Beis, D., Stainier, D.Y.R., 2006. In vivo cell biology: following the zebrafish trend. Trends Cell Biol. 16 (2), 105–112. https://doi.org/10.1016/j.tcb.2005.12.001.

Boothby, T.C., Tapia, H., Brozena, A.H., et al., 2017. Tardigrades use intrinsically disordered proteins to survive desiccation. Mol. Cell 65 (6), 975–984.e5. https://doi.org/10.1016/j.molcel.2017.02.018.

Burnett K., Edsinger E., Albrecht D.R. Hydrogel encapsulation of living organisms for long-term microscopy. Published online September 27, 2017. doi:10.1101/194282.

Coste, A., Oktay, M.H., Condeelis, J.S., Entenberg, D., 2020. Intravital imaging techniques for biomedical and clinical research. Cytom. Pt A 97 (5), 448–457. https://doi.org/10.1002/cyto.a.23963.

Cox, G.K., Gillis, T.E., 2020. Surviving anoxia: the maintenance of energy production and tissue integrity during anoxia and reoxygenation. J. Exp. Biol. 223 (13), jeb207613. https://doi.org/10.1242/jeb.207613.

Czerneková, M., Janelt, K., Student, S., Jönsson, K.I., Poprawa, I., 2018a. A comparative ultrastructure study of storage cells in the eutardigrade Richtersius coronifer in the hydrated state and after desiccation and heating stress. In: Klymkowsky, M. (Ed.), PLoS ONE, 13, e0201430. https://doi.org/10.1371/journal.pone.0201430.

Czerneková, M., Janelt, K., Student, S., Jönsson, K.I., Poprawa, I., 2018b. A comparative ultrastructure study of storage cells in the eutardigrade Richtersius coronifer in the hydrated state and after desiccation and heating stress. In: Klymkowsky, M. (Ed.), PLoS ONE, 13, e0201430. https://doi.org/10.1371/journal.pone.0201430.

Ershov, D., Phan, M.S., Pylvänäinen, J.W., et al., 2022. TrackMate 7: integrating state-of-the-art segmentation algorithms into tracking pipelines. Nat. Methods 19 (7), 829–832. https://doi.org/10.1038/s41592-022-01507-1.

Flinn, B.B., O'Dell, H.M., Joseph, K.M., et al., 2024. Fluorescence shadow imaging of Hypsibius exemplaris reveals morphological differences between sucrose- and CaCl2-induced osmobiotes. Sci. Rep. 14 (1), 11845. https://doi.org/10.1038/s41598-024-61374-y.

Giovannini, I., Boothby, T.C., Cesari, M., Goldstein, B., Guidetti, R., Rebecchi, L., 2022. Production of reactive oxygen species and involvement of bioprotectants during anhydrobiosis in the tardigrade Paramacrobiotus spatialis. Sci. Rep. 12 (1), 1938. https://doi.org/10.1038/s41598-022-05734-6.

Gómez-de-Mariscal, E., Grobe, H., Pylvänäinen, J.W., et al., 2024. CellTracksColab is a platform that enables compilation, analysis, and exploration of cell tracking data. In: Parent, C.A. (Ed.), PLoS Biol, 22, e3002740. https://doi.org/10.1371/journal.pbio.3002740.

Greenspan, P., Mayer, E.P., Fowler, S.D., 1985. Nile red: a selective fluorescent stain for intracellular lipid droplets. J. Cell Biol. 100 (3), 965–973. https://doi.org/10.1083/jcb.100.3.965.

Guidetti, R., Altiero, T., Rebecchi, L., 2011. On dormancy strategies in tardigrades. J. Insect Physiol. 57 (5), 567–576. https://doi.org/10.1016/j.jinsphys.2011.03.003.

Hagelbäck, P., Jönsson, K.I., 2023. An experimental study on tolerance to hypoxia in tardigrades. Front Physiol. 14, 1249773. https://doi.org/10.3389/fphys.2023.1249773.

Halberg, K.A., Larsen, K.W., Jørgensen, A., Ramløv, H., Møbjerg, N., 2012. Inorganic ion composition in Tardigrada: cryptobionts contain large fraction of unidentified organic solutes. Published online January 1, J. Exp. Biol., jeb.075531. https://doi.org/10.1242/jeb.075531. Published online January 1,.

Harry, C.J., Hibshman, J.D., Damatac, A., et al., 2024. Protocol for fluorescent live-cell staining of tardigrades. STAR Protoc. 5 (3), 103232. https://doi.org/10.1016/j.xpro.2024.103232.

Hashimoto, T., Horikawa, D.D., Saito, Y., et al., 2016. Extremotolerant tardigrade genome and improved radiotolerance of human cultured cells by tardigrade-unique protein. Nat. Commun. 7 (1), 12808. https://doi.org/10.1038/ncomms12808.

Hauton, D., Bennett, M.J., Evans, R.D., 2001. Utilisation of triacylglycerol and non-esterified fatty acid by the working rat heart: myocardial lipid substrate preference. Biochim. Et. Biophys. Acta (BBA) - Mol. Cell Biol. Lipids 1533 (2), 99–109. https://doi.org/10.1016/S1388-1981(01)00146-9.

Heikes, K.L., Goldstein, B., 2018. Live Imaging of Tardigrade Embryonic Development by Differential Interference Contrast Microscopy. Cold Spring Harb. Protoc. 2018 (11), pdb.prot102335. https://doi.org/10.1101/pdb.prot102335.

Hesgrove, C., Boothby, T.C., 2020. The biology of tardigrade disordered proteins in extreme stress tolerance. Cell Commun. Signal 18 (1), 178. https://doi.org/10.1186/s12964-020-00670-2.

Hyra, M., Rost-Roszkowska, M.M., Student, S., et al., 2016. Body cavity cells of Parachela during their active life. Zool. J. Linn. Soc. 178 (4), 878–887. https://doi.org/10.1111/zoj.12463.

Iessi, E., Logozzi, M., Lugini, L., et al., 2017. Acridine Orange/exosomes increase the delivery and the effectiveness of Acridine Orange in human melanoma cells: A new prototype for theranostics of tumors. J. Enzym. Inhib. Med. Chem. 32 (1), 648–657. https://doi.org/10.1080/14756366.2017.1292263.

Kasianchuk, N., Rzymski, P., Kaczmarek, Ł., 2023. The biomedical potential of tardigrade proteins: A review. Biomed. Pharmacother. 158, 114063. https://doi.org/10.1016/j.biopha.2022.114063.

Kayastha, P., Szydło, W., Mioduchowska, M., Kaczmarek, Ł., 2023. Morphological and genetic variability in cosmopolitan tardigrade species-Paramacrobiotus fairbanksi Schill, Förster, Dandekar & Wolf, 2010. Sci Rep. 13 (1), 17672. https://doi.org/10.1038/s41598-023-42653-6.

Keilin, D., 1959. The Leeuwenhoek Lecture - The problem of anabiosis or latent life: history and current concept. Proc. R. Soc. Lond. B 150 (939), 149–191. https://doi.org/10.1098/rspb.1959.0013.

Kleinhans, D.S., Lecaudey, V., 2019. Standardized mounting method of (zebrafish) embryos using a 3D-printed stamp for high-content, semi-automated confocal imaging. BMC Biotechnol. 19 (1), 68. https://doi.org/10.1186/s12896-019-0558-y.

Leyden, C., Brüggemann, T., Debinski, F., Simacek, C.A., Dehmelt, F.A., Arrenberg, A.B., 2022. Efficacy of Tricaine (MS-222) and Hypothermia as Anesthetic Agents for Blocking Sensorimotor Responses in Larval Zebrafish. Front Vet. Sci. 9, 864573. https://doi.org/10.3389/fvets.2022.864573.

Liu, Y., Dale, S., Ball, R., et al., 2019. Imaging neural events in zebrafish larvae with linear structured illumination light sheet fluorescence microscopy. Neurophoton 6 (01), 1. https://doi.org/10.1117/1.NPh.6.1.015009.

Miller, M.A., Zachary, J.F., 2017. Mechanisms and Morphology of Cellular Injury, Adaptation, and Death. In: *Pathologic Basis of Veterinary Disease*. Elsevier, p. 2. https://doi.org/10.1016/B978-0-323-35775-3.00001-1.

Møbjerg, N., Halberg, K.A., Jørgensen, A., et al., 2011. Survival in extreme environments - on the current knowledge of adaptations in tardigrades: Adaptation to extreme environments in tardigrades. Acta Physiol. 202 (3), 409–420. https://doi.org/10.1111/j.1748-1716.2011.02252.x.

Møbjerg, N., Neves, R.C., 2021. New insights into survival strategies of tardigrades. Comp. Biochem Physiol. A Mol. Integr. Physiol. 254, 110890. https://doi.org/10.1016/j.cbpa.2020.110890.

Momeni S., Phillipi E., Bushman T., et al. Armored Terrestrial Tardigrades use Cryptogam-Host Cues of Pending Environmental Deterioration to Initiate Cryptobiosis. Published online January 26, 2024. doi:10.21203/rs.3.rs-3897773/v1.

Nelson, D.R., 2002. Current Status of the Tardigrada: Evolution and Ecology. Integr. Comp. Biol. 42 (3), 652–659. https://doi.org/10.1093/icb/42.3.652.

Nunney, L., 2016. Adapting to a Changing Environment: Modeling the Interaction of Directional Selection and Plasticity. JHERED 107 (1), 15–24. https://doi.org/10.1093/jhered/esv084.

Pedersen, B.H., Malte, H., Ramløv, H., Finster, K., 2020. A method for studying the metabolic activity of individual tardigrades by measuring oxygen uptake using micro-respirometry. Published online January 1 J. Exp. Biol., jeb.233072. https://doi.org/10.1242/jeb.233072.

Perry, E.S., Miller, W.R., Lindsay, S., 2015. Looking at tardigrades in a new light: using epifluorescence to interpret structure: TARDIGRADE CUTICLE AUTOFLUORESCENCE. J. Microsc. 257 (2), 117–122. https://doi.org/10.1111/jmi.12190.

Pittet, M.J., Weissleder, R., 2011. Intravital Imaging. Cell 147 (5), 983–991. https://doi.org/10.1016/j.cell.2011.11.004.

Qian, H., Robertson, A.P., Powell-Coffman, J.A., Martin, R.J., 2008. Levamisole resistance resolved at the single-channel level in *Caenorhabditis elegans*. FASEB J. 22 (9), 3247–3254. https://doi.org/10.1096/fj.08-110502.

Quiroga-Artigas G., Moriel-Carretero M. *Storage Cell Proliferation during Somatic Growth Establishes That Tardigrades Are Not Eutelic Organisms*. Developmental Biology; 2023. doi:10.1101/2023.10.12.562009.

Reuner, A., Hengherr, S., Brümmer, F., Schill, R.O., 2010. Comparative studies on storage cells in tardigrades during starvation and anhydrobiosis. Curr. Zool. 56 (2), 259–263. https://doi.org/10.1093/czoolo/56.2.259.

Stec, D., Vecchi, M., Dudziak, M., Bartels, P.J., Calhim, S., Michalczyk, Ł., 2021. Integrative taxonomy resolves species identities within the Macrobiotus pallarii complex (Eutardigrada: Macrobiotidae). Zoological Lett. 7 (1), 9. https://doi.org/10.1186/s40851-021-00176-w.

Stefánsson, A., Arnórsson, S., Sveinbjörnsdóttir, Á.E., 2005. Redox reactions and potentials in natural waters at disequilibrium. Chem. Geol. 221 (3-4), 289–311. https://doi.org/10.1016/j.chemgeo.2005.06.003.

Suma, H.R., Prakash, S., Eswarappa, S.M., 2020. Naturally occurring fluorescence protects the eutardigrade *Paramacrobiotus* sp. from ultraviolet radiation. Biol. Lett. 16 (10), 20200391. https://doi.org/10.1098/rsbl.2020.0391.

Tanaka, S., Aoki, K., Arakawa, K., 2023a. In vivo expression vector derived from anhydrobiotic tardigrade genome enables live imaging in Eutardigrada. Proc. Natl. Acad. Sci. USA 120 (5), e2216739120. https://doi.org/10.1073/pnas.2216739120.

Tanaka, S., Aoki, K., Arakawa, K., 2023b. In vivo expression vector derived from anhydrobiotic tardigrade genome enables live imaging in Eutardigrada. Proc. Natl. Acad. Sci. USA 120 (5), e2216739120. https://doi.org/10.1073/pnas.2216739120.

Tattersall G.J., Sinclair B.J., Withers P.C., et al. Coping with Thermal Challenges: Physiological Adaptations to Environmental Temperatures. In: Prakash YS, ed. Comprehensive Physiology. 1st ed. Wiley; 2012:2151-2202. doi:10.1002/cphy.c110055.

Wilson, T., 2010. Spinning-Disk Microscopy Systems. Cold Spring Harb. Protoc. 2010 (11), pdb.top88. https://doi.org/10.1101/pdb.top88.

Wilsterman, K., Ballinger, M.A., Williams, C.M., 2021. A unifying, eco-physiological framework for animal dormancy. In: Lemaître, J. (Ed.), Functional Ecology, 35, pp. 11–31. https://doi.org/10.1111/1365-2435.13718.